# Demonstration of a Coupled Watershed-Nearshore Model

*by Hwai-Ping Cheng, Jing-Ru C. Cheng, Robert M. Hunter, and Hsin-Chi Lin*

**PURPOSE:** This technical note documents a research demonstration of a newly-developed watershed-nearshore computational model, which couples the **p**arallel **WA**ter**SH**ed systems of one-dimensional (**1**-D) stream-river networks, two-dimensional (**2**-D) overland regimes, and three-dimensional (**3**-D) subsurface media (pWASH123D) model with the 2-D **AD**vanced **CIRC**ulation model for oceanic, coastal, and estuarine waters (ADCIRC). This task was sponsored by the System-Wide Water Resources Program (SWWRP). It was conducted through the simulation of water flow in a simplified Biloxi Bay hydro-system.

**BACKGROUND:** Coupling pWASH123D (Cheng et al. 2006, 2007) and 2-D ADCIRC (ADCIRC 2009) using the Earth System Modeling Framework (ESMF) (ESMF 2009) is the task of the BEI-04 project in the Battlespace Environments Institute (BEI) that is sponsored by the DoD High Performance Computing Modernization Program (Department of Defense 2010). The two models are coupled in a concurrent mode with time lagging, where the ESMF and DBuilder (Hunter and Cheng 2006) are used to provide the software architecture and parallel data management, including all the functional support of data exchange between the two models. The coupled model passed the beta test, where four critical technical parameters, including accuracy, portability, integration, and scalability, were examined according to the development and evaluation plan. This technical note presents the coupled model through a test example, where a simplified watershed and nearshore hydro-system around the Biloxi Bay area in Mississippi was considered. This Biloxi Bay model, constructed with the DoD Groundwater Modeling System (GMS) (USACE 2009), used historical data as well as the simulation results from a large-scale 2-D ADCIRC that modeled the 2005 hurricane Katrina as the driving forces for water movement.

**pWASH123D.** pWASH123D is the parallel version of the WASH123D model that is a physically-based finite element numerical model computing water flow within watershed systems that can be simulated as combinations of 1-D channel networks, 2-D overland regimes, and 3-D subsurface media (Yeh et al. 2006). The interactions between different modeled media (i.e., between channel and overland and between surface and subsurface) impose flux continuity and state variable continuity on the medium interfaces. The pWASH123D model aims to efficiently simulate the medium- to large-scale problems on HPC machines. Different parallel algorithms and partitioning strategies are implemented in different computational components (e.g., 1-D channel flow, 2-D overland flow, and 3-D subsurface flow) to maintain load balance and reduce communication overhead (Cheng et al. 2007). The model is a mixed C, Fortran, and C++ parallel code (Cheng et al. 2006).

| Report Documentation Page | | Form Approved OMB No. 0704-0188 |
|---|---|---|

Public reporting burden for the collection of information is estimated to average 1 hour per response, including the time for reviewing instructions, searching existing data sources, gathering and maintaining the data needed, and completing and reviewing the collection of information. Send comments regarding this burden estimate or any other aspect of this collection of information, including suggestions for reducing this burden, to Washington Headquarters Services, Directorate for Information Operations and Reports, 1215 Jefferson Davis Highway, Suite 1204, Arlington VA 22202-4302. Respondents should be aware that notwithstanding any other provision of law, no person shall be subject to a penalty for failing to comply with a collection of information if it does not display a currently valid OMB control number.

| 1. REPORT DATE **APR 2010** | 2. REPORT TYPE | 3. DATES COVERED **00-00-2010 to 00-00-2010** |
|---|---|---|
| 4. TITLE AND SUBTITLE **Demonstration of a Coupled Watershed-Nearshore Model** | | 5a. CONTRACT NUMBER |
| | | 5b. GRANT NUMBER |
| | | 5c. PROGRAM ELEMENT NUMBER |
| 6. AUTHOR(S) | | 5d. PROJECT NUMBER |
| | | 5e. TASK NUMBER |
| | | 5f. WORK UNIT NUMBER |
| 7. PERFORMING ORGANIZATION NAME(S) AND ADDRESS(ES) **U.S. Army Engineer Research and Development Center,Vicksburg,MS** | | 8. PERFORMING ORGANIZATION REPORT NUMBER |
| 9. SPONSORING/MONITORING AGENCY NAME(S) AND ADDRESS(ES) | | 10. SPONSOR/MONITOR'S ACRONYM(S) |
| | | 11. SPONSOR/MONITOR'S REPORT NUMBER(S) |

12. DISTRIBUTION/AVAILABILITY STATEMENT
**Approved for public release; distribution unlimited**

13. SUPPLEMENTARY NOTES

14. ABSTRACT

15. SUBJECT TERMS

| 16. SECURITY CLASSIFICATION OF: | | | 17. LIMITATION OF ABSTRACT | 18. NUMBER OF PAGES | 19a. NAME OF RESPONSIBLE PERSON |
|---|---|---|---|---|---|
| a. REPORT **unclassified** | b. ABSTRACT **unclassified** | c. THIS PAGE **unclassified** | **Same as Report (SAR)** | **26** | |

**Standard Form 298 (Rev. 8-98)**
Prescribed by ANSI Std Z39-18

**ADCIRC.** The ADCIRC model is a coastal circulation and storm surge model. It is a system of finite element computer programs for solving time dependent, free surface circulation and transport problems in two and three dimensions. The model implements the continuous Galerkin finite element method based on the Generalized Wave Continuity Equation (GWCE). It is a parallel Fortran 90 code. Typical ADCIRC applications have included: (a) modeling tides and wind driven circulation, (b) analysis of hurricane storm surge and flooding, (c) dredging feasibility and material disposal studies, (d) larval transport studies, and (e) near shore marine operations. For the model coupling in BEI-04, the two-dimension version of ADCIRC is employed.

**ESMF.** The ESMF is computer software for building and coupling weather, climate, and related models. It provides and defines a software architecture for composing complex, coupled modeling systems and includes data structures and utilities for developing individual models. It consists of a superstructure that can be assembled into user applications and an infrastructure for building model components. It was originally funded by the National Aeronautics and Space Administration (NASA) to support climate and weather modeling. The ESMF effort then brought together different areas of research funding to extend its support to diverse modeling works. It is the designated tool to conduct model coupling in the BEI. Sponsored by BEI, the ESMF has been developing its unstructured mesh functionality. The coupling of pWASH123D and 2-D ADCIRC is the first application of unstructured mesh in ESMF. Although the coupled model has used DBuilder for data exchange through the coupling interface, the ESMF unstructured mesh functionality has been developing. The ESMF is still used for startup, oversight of model runtime, and completion of the coupled model (Figure 1). The developed ESMF unstructured mesh support is now tested and incorporated into the coupled pWASH123D-ADCIRC model in the BEI-04 project.

**DBuilder.** The DBuilder toolkit is a parallel data management library for scientific applications, which is currently used to facilitate the data exchange between the two models (Hunter and Cheng 2005). It has been developed to assist developers in implementing parallel versions of their codes by providing a simple, consistent application programming interface (API) that hides many of the programming details associated with domain partitioning, parallel data management, domain coupling, and invoking parallel linear solvers. Because DBuilder supports coupling independent domains in a single model (i.e., pWASH123D's 1-D, 2-D, and 3-D domains), adopting it to exchange data between models was not a large task. It was used in the coupled model because the ESMF was lacking support for unstructured meshes at the time of initial development.

**DoD GMS.** GMS is one of the most sophisticated groundwater modeling environments available today. It provides an integrated and comprehensive computational environment for simulating subsurface flow, contaminant fate/transport, and the efficacy and design of remediation systems. It also provides a comprehensive graphical environment for numerical modeling, tools for site characterization, model conceptualization, mesh and grid generation, geo-statistics, and sophisticated tools for graphical visualization. There is a pWASH123D graphic user interface included in GMS 6.5. In this demonstration task, GMS was also used to generate the ADCIRC mesh. The generated geometry file was later converted to the ADCIRC format.
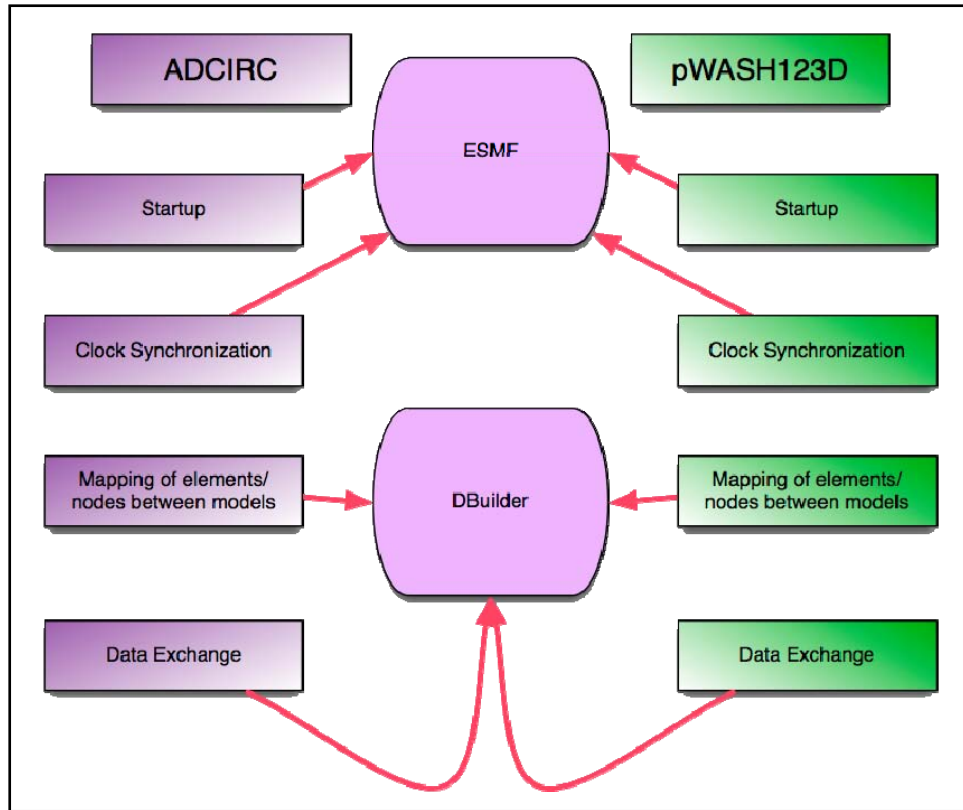
Figure 1. The implementation strategy for the coupled pWASH123D-ADCIRC model.

**METHODOLOGY:** Figure 2 shows the diagram of data exchange between pWASH123D and 2-D ADCIRC in the coupled model. Through the coupling interface, the computed water surface elevation from 2-D ADCIRC is used as a Dirichlet-type boundary condition for pWASH123D computation, while the mass flow computed from pWASH123D is used as a flux-type boundary condition for 2-D ADCIRC computation.
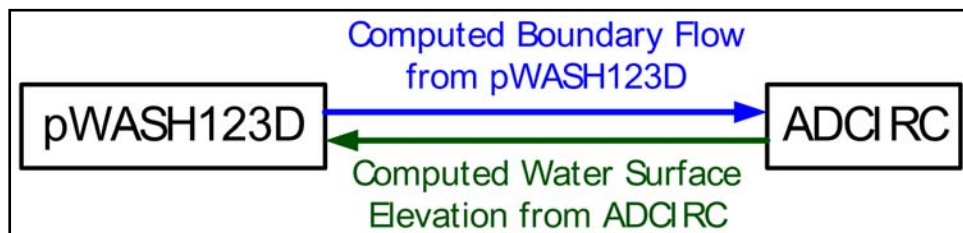


Figure 2. Data exchange in the coupled pWASH123D-ADCIRC model.

The ESMF requires that a model application code consists of three distinct phases: initialize, run, and finalize. The application developer needs to implement a main program including the three phases, in which some ESMF functions are called (Figure 3). We will call this file COSM.f. A user would then create an interface file that contains the three functions (initialize, run, and finalize) for a particular model. For this example, we will call them pWASH123.c and ADCIRC.f. The last piece the user needs to implement is a coupler component. This component contains coupler initialization routines, which may be used to create import and export states

3

containing scalars and vectors for data exchange. The coupler component, which is named Coupler.f here, also contains the run routine that executes the designated coupling algorithms and a finalize routine.
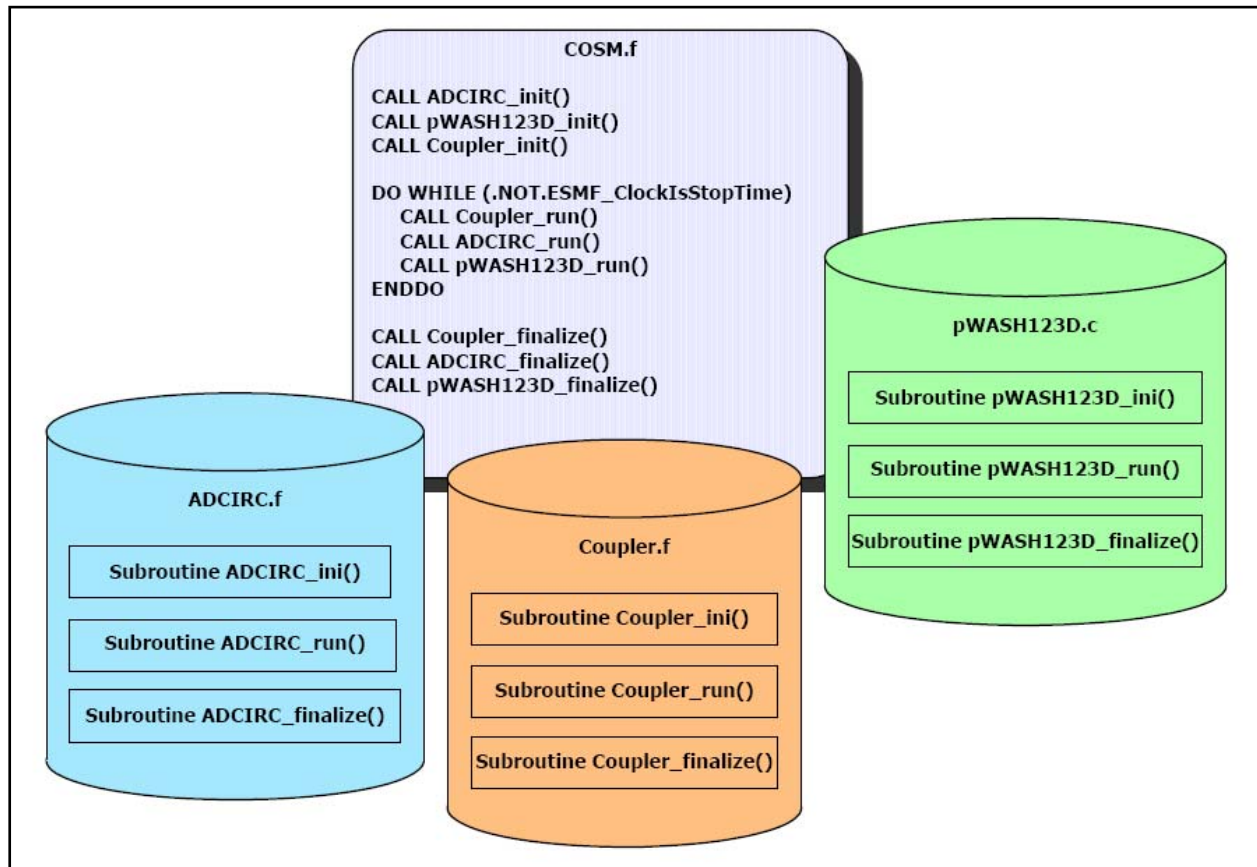


Figure 3. ESMF coupling and coupler components.

In the current implementation of the coupled pWASH123D-ADCIRC model, the coupler component relies on the functionality of DBuilder for implementation of the coupler "init" and coupler runtime routines. The coupler contains a key component provided by DBuilder, which is an element searching routine. When the models are run, there is no static information with regard to the mapping of nodes to elements along the boundary interface of the two models. This interface boundary may also be an overlapped region. At runtime each model determines its interface nodes based upon its own boundary condition values. Then in the coupler initialization routine, each model passes the geometric coordinates of its interface nodes to the other model. The element searching routine is then called on each model to build a list of elements containing the coordinates from the other model.

One should keep in mind that this is all done in parallel over already partitioned meshes in both models. The element searching algorithm is constructed using an Alternating Digital Tree (ADT) (Bonet and Peralie 2005) with a complexity of O (log N), where N is the number of elements. Once the element has been determined, weights are calculated for each associated node of the element. These weights are the nodal contribution from each node to the value calculated at the

geometric coordinate. The computed value is then shipped back to the model processor that owns the node.

**Data Exchange through Coupling Interface.** The current coupling approach uses the coastal (shore) line as the coupling interface. Figure 4 depicts a side view perpendicular to the coupling interface. The current coupling requires the minimum water depth option in ADCIRC to be activated. In other words, the wetting-drying scenario is not handled at this point. To ensure the applicability of this option, an elevation drop from pWASH123D to ADCIRC on the interface boundary is enforced, as shown in Figure 4. The water surface elevation on the coupling interface that ADCIRC simulates is used as the boundary condition for computing channel flow and overland flow in the surface water system. With the hydrostatic assumption applied to each horizontal location on the coupling interface, this computed surface elevation is distributed to the subsurface nodes beneath the coastal line for computing subsurface flow. On the other hand, the boundary flow associated with all of the pWASH123D nodes on the coupling interface are computed and then distributed to the ADCIRC boundary nodes on the coupling interface. The pWASH123D boundary nodal flow includes contributions from both surface and subsurface flow. In Figure 4, f1 represents the boundary flux due to surface flow, and f2 the subsurface flow. In reality, part of f2 passes through Zone A and enters/exits the ADCIRC model across the bathymetry line as sinks/sources. In this case, Zone A should be included in the modeled domain. The current coupling approach, however, simplifies this situation by taking f2 (i.e., the subsurface contribution) at the ADCIRC boundary nodes on the coupling interface.
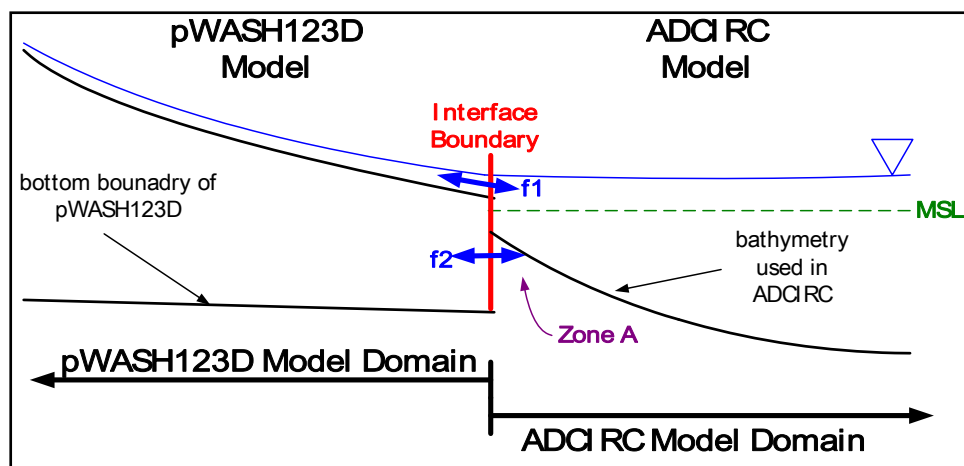


Figure 4. A side view of the coupled pWASH123D-ADCIRC model.

Element searching is essential for exchanging data when pWASH123D and ADCIRC are allowed to have different mesh resolutions on the coupling interface. Figure 5 explains the algorithm used in the coupler for data exchange. The left plot depicts how the computed water surface elevation from ADCIRC is passed to pWASH123D as the head-type boundary condition on the coupling interface. In the left plot, the weights of interpolation, e.g., $N_{1i}$, $N_{2i}$, $N_{3i}$, are computed after element searching, where pWASH123D node **i** is found in an ADCIRC element comprising nodes 1, 2, and 3. With the computed weights of interpolation for all of the pWASH123D nodes on the coupling interface, the right plot shows how the pWASH123D boundary nodal flow

is distributed to the associated ADCIRC boundary node to form flux-type boundary conditions on the coupling interface.
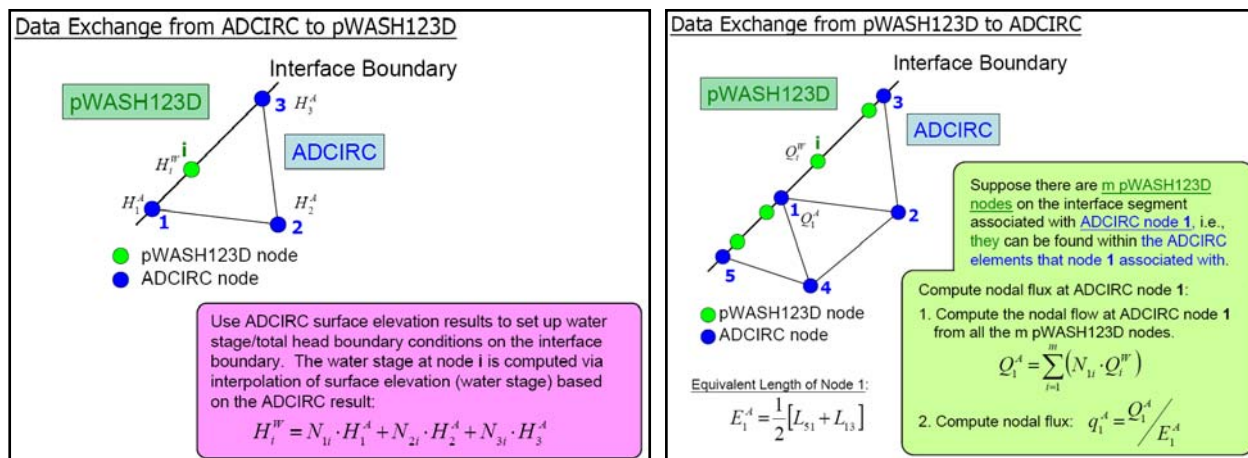


Figure 5. Data exchange algorithms used in the coupler of the coupled model.

**Concurrent Mode with Time Lagging.** As shown in Figure 6, pWASH123D and ADCIRC are currently coupled in a concurrent mode with time lagging. At each coupling time-step, ADCIRC and pWASH123D uses the computed average boundary flux (Qavg) and water surface elevation (H), both computed from the previous coupling time-step, as the boundary condition on the coupling interface. Because of the use of the computed values from the previous time-step for setting up the boundary conditions on the coupling interface, a time lagging effect exists in the current coupling mode. The coupled simulation will not proceed to the next coupling time-step until both pWASH123D and ADCIRC have completed their computations within one coupling time-step.

It is noted that the current coupling of pWASH123D and ADCIRC requires the coupling time-step to be a common multiple of the ADCIRC time-step and the pWASH123D subsurface time-step. In the pWASH123D simulation, it is required that the subsurface time-step is a multiple of the overland time-step and that the overland time-step is a multiple of the channel time-step. As a result, the coupling time-step is a common multiple of the time-steps for ADCIRC, 1-D channel, 2-D overland, and 3-D subsurface computation.

**DEMONSTRATION EXAMPLE:** A simplified Biloxi model was developed and used to demonstrate the coupled pWASH123D-ADCIRC model. Detailed ADCIRC modeling has been done for Hurricanes Katrina and Rita and extensively validated using a large set of measured data (Bunya et al. 2010a, 2010b). While not suitable for highly detailed and accurate storm surge simulations, the ADCIRC mesh used in this study is appropriate and adequate for the purposes of this work, which is focused on test and evaluation of different approaches to couple ADCIRC and the surface-subsurface model pWASH123D. The domain of this simplified Biloxi model includes an area covering the downstream Biloxi River watershed in Mississippi (the pWASH123D domain, ~$6.9 \times 10^8$ m$^2$) and an extended Biloxi Bay area (the ADCIRC domain, ~$3.0 \times 10^9$ m$^2$), as sketched in Figure 7. The blue lines in the figure represent both rivers/streams and coastal lines, while the right plot shows the topographic/bathymetric variation within the domain. The coastal line serves as the coupling interface between ADCIRC and pWASH123D.
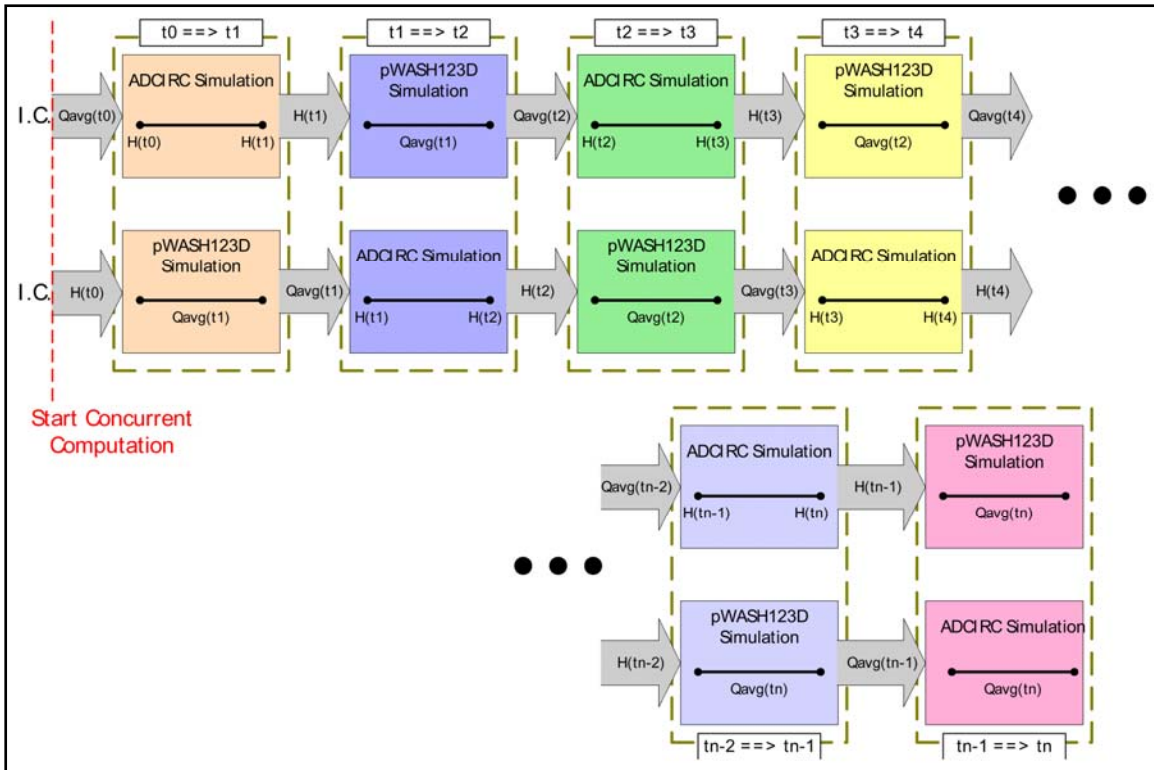
6

Figure 6.   The concurrent mode with time lagging used for the coupled pWASH123D-ADCIRC model.
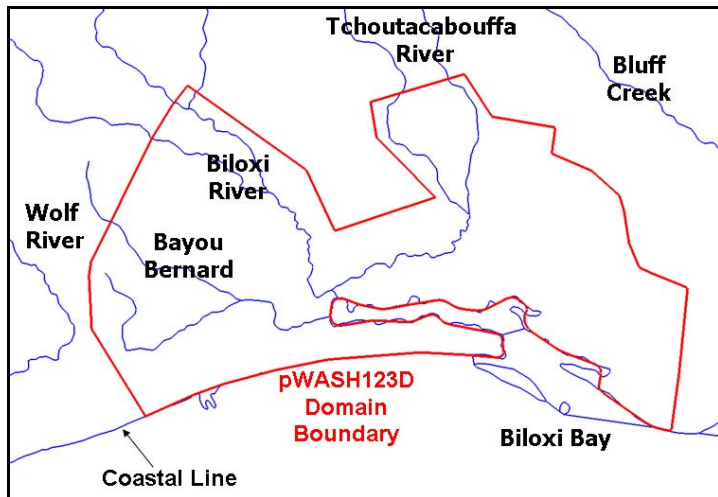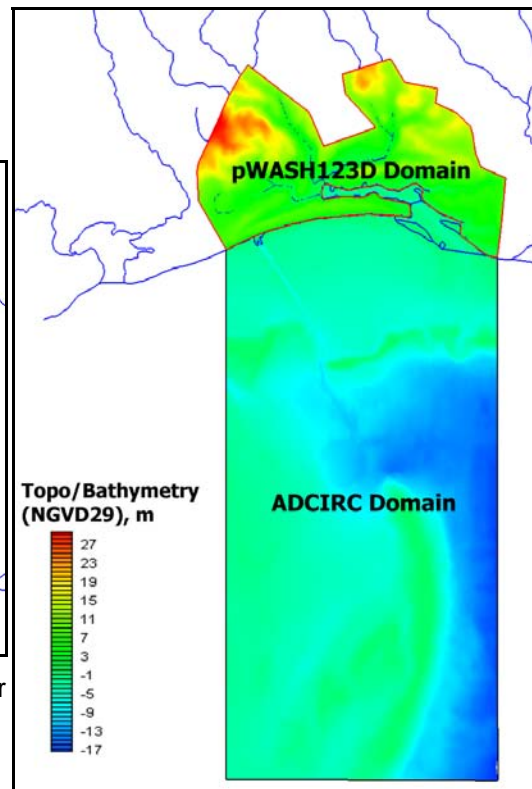


Figure 7.   Biloxi model domain: the downstream Biloxi River watershed in Mississippi and an extended Biloxi Bay area.

7

**Model Construction.** In general, the ADCIRC domain must be large enough to cover the evolution of the storm/hurricane. The ADCIRC domain shown in Figure 7 is too small to simulate the Hurricane Katrina event effectively if wind stress is the only driving force applied. To overcome this difficulty without including a large-scale ADCIRC domain in the coupled model, we used the computed water surface elevation from a large-scale ADCIRC model to construct the boundary condition on the open boundary. This large-scale ADCIRC model was generated and calibrated using the field data provided by the research group of Professor Shahrouz Aliabadi at Jackson State University (JSU), MS. Figure 8 shows the JSU large-scale ADCIRC model (lower left plot) as well as the ADCIRC mesh of the Biloxi model (upper left plot), which is composed of 20,601 nodes and 40,470 elements. The JSU large-scale ADCIRC model simulated the Hurricane Katrina event over a 7-day time period until it made landfall on the Gulf Coast, where the wind stress data from NOAA were employed. Our demonstration here considered a 72-hour simulation starting from 1800 GMT August 27 to 1800 GMT August 30, 2005, where the storm surge peaked at around 1400 GMT August 29, 2005 at the west end of the coupling interface (i.e., simulation time = 44 hr), which is marked with a red "A" in the upper left plot of Figure 8.

Due to time and resource constraints, the pWASH123D model constructed for this Biloxi model employed a simplified channel network (Figure 9), imposed homogeneity to both the overland and subsurface systems, and used synthetic rainfall data to set up the model runs. Although the model was not calibrated, it can be used to examine the coupling performance in BEI-04. Figure 10 shows the pWASH123D mesh that is composed of 301 nodes and 291 elements for 1-D channel flow, 15,005 nodes and 18,982 elements for 2-D overland flow, and 105,035 nodes and 173,892 elements for 3-D subsurface flow computation. A sensitivity analysis on spatial and temporal resolution was conducted to determine the final pWASH123D mesh and time-step sizes for this study.

The pWASH123D model boundary on the land side was selected based on the topographical contour, such that drainage divide can be assumed and no-flow boundary conditions can be applied there. Figure 11 gives an overview of the boundary conditions employed in the coupled model. The time-steps used for the base-case run were: 1 sec for the 2-D ADCIRC computation, 0.5 sec for 1-D channel flow, 5 sec for 2-D overland flow, 6 min for 3-D subsurface flow, and 6 min for coupling.
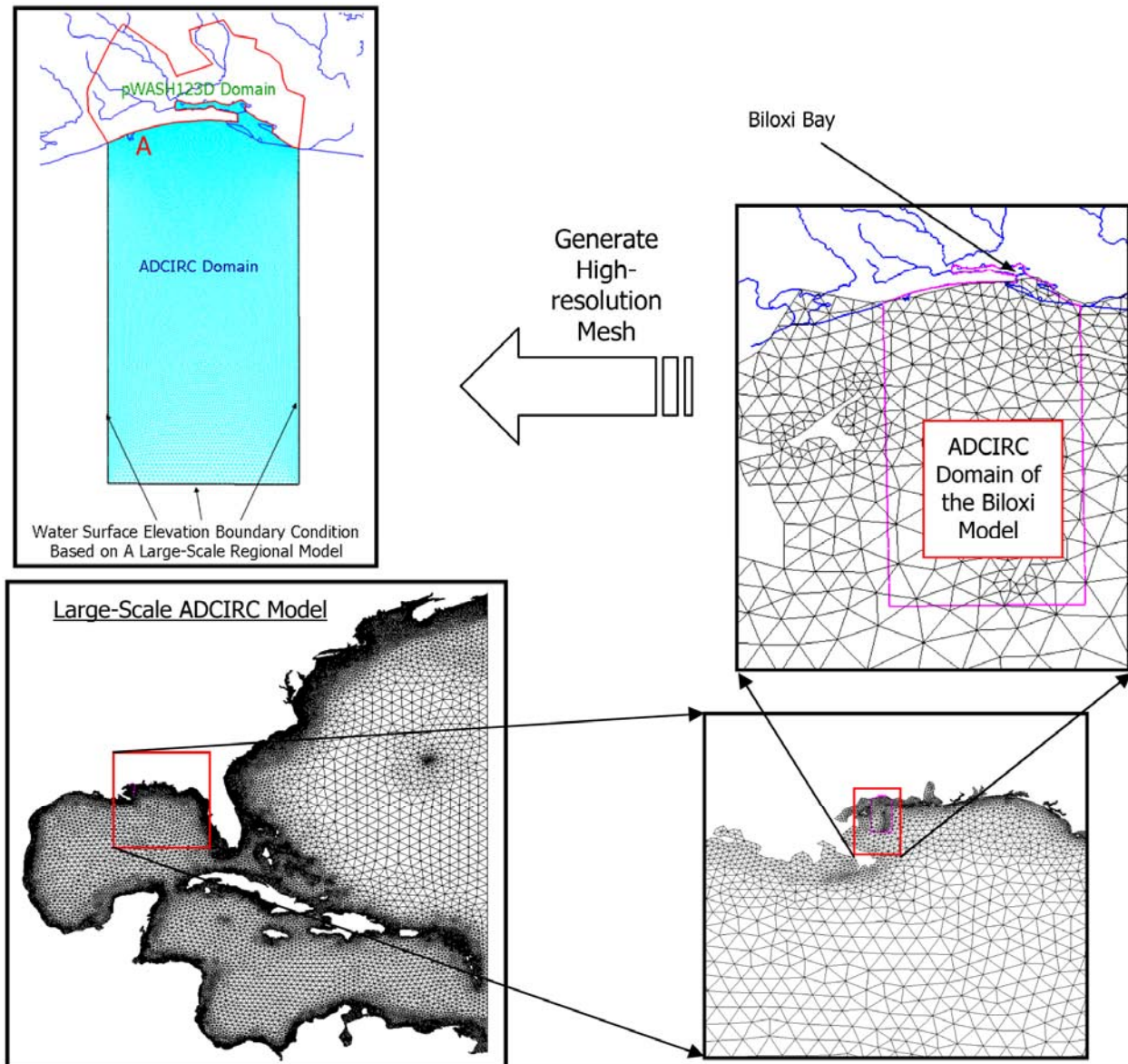
Figure 8.    From the large-scale ADCIRC model (left plot) to the ADCIRC domain (labeled in the upper right plot) of the Biloxi model.
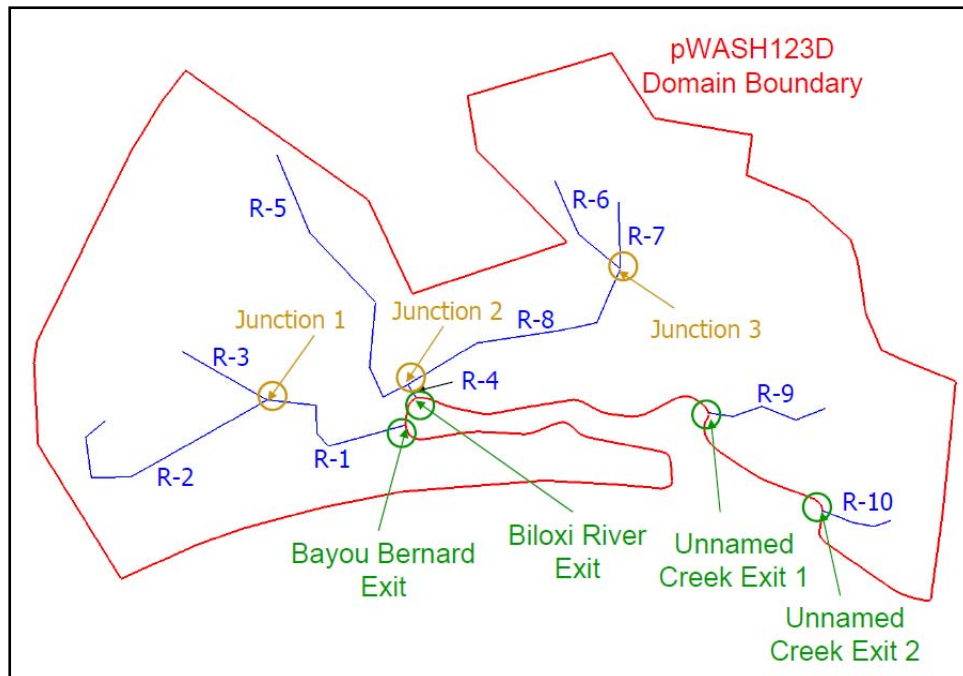
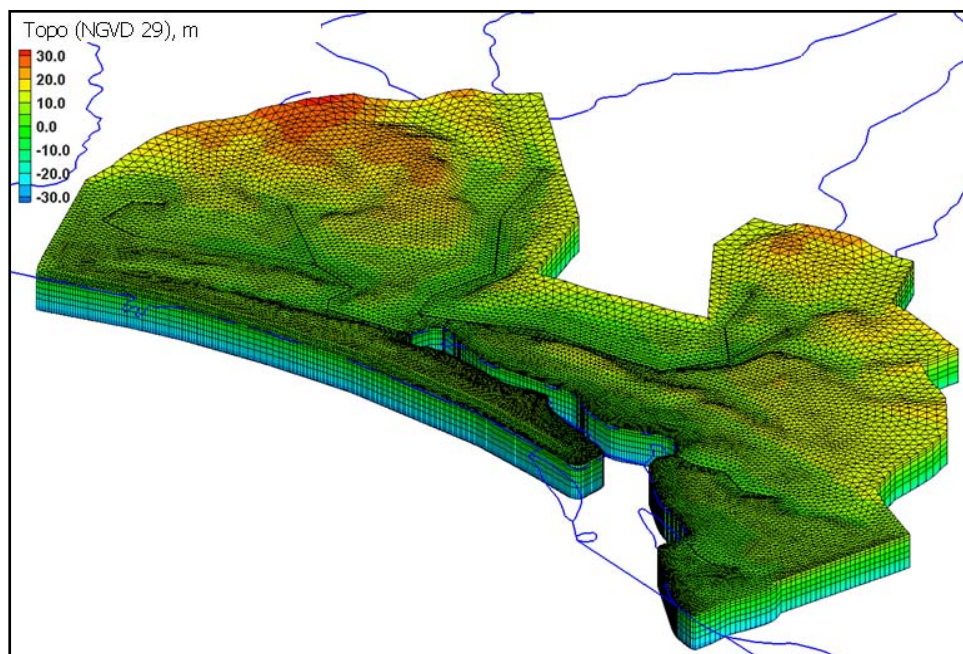Figure 9. Simplified channel network in the Biloxi model.



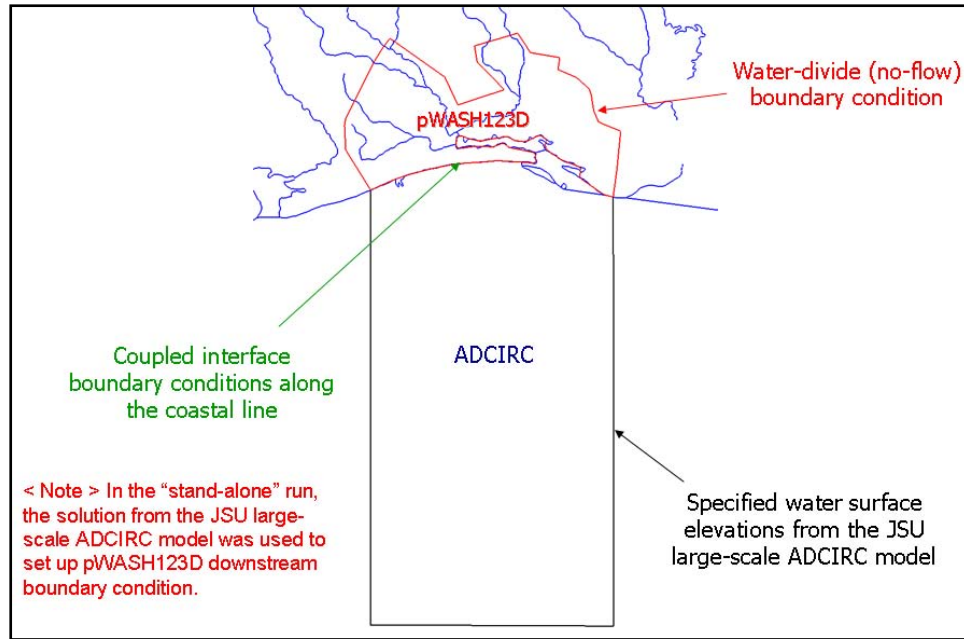Figure 10. The pWASH123D mesh in the Biloxi model.

Figure 11. Boundary conditions for the coupled model.

Table 1 lists the 38 model runs conducted in this research demonstration to examine various aspects of the coupled model, including the scalability performance, the accuracy performance, the coupling scheme effect, the time lagging effect, and the hydraulic conductivity effect. All of the model runs were conducted on a Cray XT3 (Carbon, ERDC). These 38 model runs include stand-alone (light green shading), one-way coupling (light blue shading), and two-way coupling (yellow shading) simulations. They are defined as follows:

(1) Stand-alone simulation: either the ADCIRC or the pWASH123D run was conducted.

(2) One-way coupling simulation: the computed water surface elevation from ADCIRC was passed to pWASH123D as the boundary condition on the coupling interface.

(3) Two-way coupling simulation: in addition to the data transfer from ADCIRC to pWASH123D, the computed boundary flux along the coupling interface from pWASH123D was passed to ADCIRC.

A no-flow boundary condition was applied to the coastal line (i.e., the coupling interface) in the ADCIRC stand-alone simulation. The computed water surface elevation from the JSU large-scale ADCIRC model was used to set up the boundary condition along the coastal line in the pWASH123D stand-alone simulation.

**Table 1. Wall clock time of the 34 model runs conducted in the research demonstration.**

| Run ID | No of Proc. pWASH123D | No of Proc. ADCIRC | Wall Clock Time (s) | PE (%)[+] | Simulation Type |
|---|---|---|---|---|---|
| 1 | 0 | 2 | 10,230 | Baseline | ADCIRC stand alone |
| 2 | 0 | 4 | 4,335 | 117.99% | |
| 3 | 0 | 8 | 2,624 | 97.47% | |
| 4 | 0 | 16 | 1,867 | 68.49% | |
| 5 | 8 | 0 | 15,378 | Baseline | pWASH123D stand alone |
| 6 | 16 | 0 | 9,316 | 82.54% | |
| 7 | 32 | 0 | 7,411 | 51.88% | |
| 8 | 64 | 0 | 7,559 | 25.43% | |
| 9 | 8 | 0 | 19,672 | Baseline | pWASH123D stand alone $\Delta t_{subsurface}$ = 3 min |
| 10 | 16 | 0 | 12,369 | 79.52% | |
| 11 | 32 | 0 | 10,205 | 48.19% | |
| 12 | 64 | 0 | 10,996 | 22.36% | |
| 13 | 32 | 2 | 18,094 | Baseline | Two-Way Coupling |
| 14 | 32 | 4 | 9,092 | 99.51% | |
| 15 | 32 | 8 | 5,408 | 83.64% | |
| 16 | 32 | 16 | 5,067 | 44.64% | |
| 17 | 32 | 2 | 18,285 | Baseline | Two-Way Coupling, high K (x10) $\Delta t_{subsurface}$ = 3 min, $\Delta t_{coupling}$ = 3 min |
| 18 | 32 | 4 | 9,095 | 100.52% | |
| 19 | 32 | 8 | 7,439 | 61.45% | |
| 20 | 32 | 16 | 7,650 | 29.88% | |
| 21 | 32 | 2 | 19,704 | Baseline | Two-Way Coupling, low K (x0.1) $\Delta t_{subsurface}$ = 3 min, $\Delta t_{coupling}$ = 3 min |
| 22 | 32 | 4 | 10,516 | 93.69% | |
| 23 | 32 | 8 | 7,086 | 69.52% | |
| 24 | 32 | 16 | 6,613 | 37.24% | |
| 25 | 32 | 8 | 6,107 | N/A | Two-Way Coupling, $\Delta t_{subsurface}$ = 3 min |
| 26 | 32 | 2 | 18,284 | Baseline | Two-Way Coupling, $\Delta t_{subsurface}$ = 3 min, $\Delta t_{coupling}$ = 3 min |
| 27 | 32 | 4 | 9,100 | 100.46% | |
| 28 | 32 | 8 | 5,921 | 77.20% | |
| 29 | 32 | 16 | 6,078 | 37.60% | |
| 30 | 32 | 8 | 6,667 | N/A | One-Way Coupling, $\Delta t_{subsurface}$ = 3 min |
| 31 | 32 | 2 | 11,143 | Baseline | One-Way Coupling, $\Delta t_{subsurface}$ = 3 min, $\Delta t_{coupling}$ = 3 min |
| 32 | 32 | 4 | 6,931 | 80.39% | |
| 33 | 32 | 8 | 6,923 | 40.24% | |
| 34 | 32 | 16 | 6,844 | 20.35% | |
| 35 | 8 | 8 | 11,430 | Baseline | Two-Way Coupling |
| 36 | 16 | 8 | 6,812 | 83.90% | |
| 37 | 32 | 8 | 5,408 | 52.84% | |
| 38 | 64 | 8 | 4,943 | 28.90% | |

\* Time-steps for base case simulation: $\Delta t_{ADCIRC}$ = 1 s; $\Delta t_{channel}$ = 0.5 s; $\Delta t_{overland}$ = 5 s; $\Delta t_{subsurface}$ = 6 min; $\Delta t_{coupling}$ = 6 min

\*\* Hydraulic conductivities for base case simulation: 10 m/hr (horizontal) and 1 m/hr (vertical) along channels, and 100 m/hr (horizontal) 10 m/hr (vertical) elsewhere

[+] PE = parallel efficiency = $\left( NP_{baseline} \cdot T_{baseline} \right) / \left( NP_{comparison} \cdot T_{comparison} \right) \cdot 100\%$

## RESULTS.

**Scalability performance.** Table 1 lists the wall clock times and the computed parallel efficiency (PE) for the 38 model runs, where PE is defined in the footnote of Table 1. Each of the 38 runs was conducted twice, and the average wall clock times were put in Table 1. The number of the pWASH123D processor is fixed at 32 for all of the one-way and two-way coupling runs, except for the last four runs (i.e., Runs 35 – 38). From Table 1, we observe (1) the PE value of the ADCIRC stand-alone simulation is greater than 95 percent up to eight processors; (2) the PE value of the pWASH123D stand-alone simulation is greater than 77 percent up to 16 processors; (3) the PE value of the one-way coupling simulation is greater than 79 percent up to four ADCIRC processors; (4) the PE value of the two-way coupling simulation is greater than 93 percent up to four ADCIRC processors and 63 percent up to eight ADCIRC processors; (5) using 32 pWASH123D processors and eight ADCIRC processors seems to be the best combination for the designated 72-hour simulation when both the PE and wall clock time lengths are considered.

**Accuracy performance.** Tables 2 through 4 compare model run results when different numbers of processors are used. The model run results include hourly solutions from zero to 30 hr, every 0.1 hour from 30 to 60 hr, and hourly again from 60 to 72 hr. In total, there are 342 time-step solutions included. Table 2 lists the comparison of 1-D channel stages, while Tables 3 and 4 are comparisons of the 2-D overland water depth and the ADCIRC water surface elevation, respectively. Four types of deviation measures were employed for comparison: Average Mean Absolute Deviation (AMAD), Average Root Mean Square Deviation (ARMSD), Average Coefficient Of Efficiency (ACOE), and Average Coefficient Of Determination (ACOD). They are defined as follows:

$$AMAD = \frac{\sum_{it=1}^{n_t} \left( \dfrac{\sum_{i=1}^{n} \left| C_{it,i} - R_{it,i} \right|}{n} \right)}{n_t} \tag{1}$$

$$ARMSD = \frac{\sum_{it=1}^{n_t} \left( \sqrt{\dfrac{\sum_{i=1}^{n} \left| C_{it,i} - R_{it,i} \right|^2}{n}} \right)}{n_t} \tag{2}$$

$$ACOE = \frac{\sum_{it=1}^{n_t} \left( 1 - \dfrac{\sum_{i=1}^{n} (R_{it,i} - C_{it,i})^2}{\sum_{i=1}^{n} (R_{it,i} - \overline{R}_{it})^2} \right)}{n_t} \tag{3}$$

$$ACOD = \frac{\sum\limits_{it=1}^{n_t}\left[\dfrac{\sum\limits_{i=1}^{n}(C_{it,i}-\overline{C}_{it})(R_{it,i}-\overline{R}_{it})}{\sqrt{\sum\limits_{i=1}^{n}(C_{it,i}-\overline{C}_{it})^2}\sqrt{\sum\limits_{i=1}^{n}(R_{it,i}-\overline{R}_{it})^2}}\right]^2}{n_t} \qquad (4)$$

where $n$ = the number of comparisons between the values from the reference and the comparative groups, both are computed here, within each time-step ; $n_t$ = the number of time-steps included for data comparison; $c_{it,i}$ = the i-th value for comparison from the comparative group that is associated with the it-th time-step; $R_{it,i}$ = the i-th value for comparison from the reference group that is associated with the i-th time-step; $\overline{C}_{it}$ = the mean value over $n$ comparisons in the comparative group at the it-th time-step; and $\overline{R}_{it}$ = the mean value over $n$ comparisons in the reference group at the it-th time-step. Basically, the two groups of data are in close agreement when *AMAD* and *ARMSD* are small and *ACOE* and *ACOD* are close to unity, or (*1 – ACOE*) and (*1 –ACOD*) are close to zero.

It is observed from Tables 2 through 4 that both (*1 – ACOE*) and (*1 –ACOD*) are close to zero in all comparisons, and that *AMAD* and *ARMSD* are small. The values of the deviation measures shown in these three tables indicate that the coupled pWASH123D-ADCIRC model provides consistent computational results in stand-alone, one-way coupling, and two-way coupling simulations when the number of processors varies.

**Table 2. Comparison statistics of the computed 1-D channel stage ($n$ = 301 and $n_t$ = 342)**

| Comparison ID | Compared Model Runs | | 1-ACOD | 1-ACOE | ARMSD, m | AMAD, m |
| --- | --- | --- | --- | --- | --- | --- |
| | Reference Run | Comparative Run | | | | |
| SA1 | Run 11 | Run 9 | 2.60E-05 | 5.90E-05 | 1.79E-04 | 1.00E-04 |
| SA2 | Run 11 | Run 10 | 2.80E-05 | 6.20E-05 | 1.83E-04 | 1.01E-04 |
| SA3 | Run 11 | Run 12 | 3.80E-05 | 8.70E-05 | 2.09E-04 | 1.18E-04 |
| SA4 | Run 7 | Run 5 | 1.20E-05 | 2.50E-05 | 1.23E-04 | 6.15E-05 |
| SA5 | Run 7 | Run 6 | 4.20E-05 | 9.40E-05 | 2.43E-04 | 1.37E-04 |
| SA6 | Run 7 | Run 8 | 5.70E-05 | 1.44E-04 | 3.38E-04 | 1.96E-04 |
| 1Way1 | Run 33 | Run 31 | 3.10E-05 | 6.30E-05 | 2.27E-04 | 1.08E-04 |
| 1Way2 | Run 33 | Run 32 | 3.00E-05 | 6.50E-05 | 2.28E-04 | 1.21E-04 |
| 1Way3 | Run 33 | Run 34 | 3.90E-05 | 8.20E-05 | 2.76E-04 | 1.40E-04 |
| 2Way1 | Run 28 | Run 26 | 1.15E-04 | 3.07E-04 | 1.99E-03 | 1.43E-03 |
| 2Way2 | Run 28 | Run 27 | 7.20E-04 | 2.09E-03 | 4.99E-03 | 3.56E-03 |
| 2Way3 | Run 28 | Run 29 | 3.89E-04 | 1.11E-03 | 4.11E-03 | 3.01E-03 |
| 2Way4 | Run 15 | Run 13 | 1.01E-04 | 3.28E-04 | 1.29E-03 | 9.73E-04 |
| 2Way5 | Run 15 | Run 14 | 5.40E-04 | 1.70E-03 | 3.22E-03 | 2.47E-03 |
| 2Way6 | Run 15 | Run 16 | 1.63E-04 | 5.24E-04 | 1.73E-03 | 1.29E-03 |

**Table 3. Comparison statistics of the computed 2-D overland water depth ($n$ = 15,005 and $n_t$ = 342)**

| Comparison ID | Compared Model Runs | | 1-ACOD | 1-ACOE | ARMSD | AMAD |
| | Reference Run | Comparative Run | | | | |
|---|---|---|---|---|---|---|
| SA1 | Run 11 | Run 9 | 5.70E-09 | 1.16E-08 | 4.52E-05 | 8.42E-06 |
| SA2 | Run 11 | Run 10 | 4.86E-09 | 9.86E-09 | 4.26E-05 | 7.91E-06 |
| SA3 | Run 11 | Run 12 | 2.03E-06 | 4.09E-06 | 7.63E-05 | 1.15E-05 |
| SA4 | Run 7 | Run 5 | 2.41E-09 | 4.87E-09 | 3.14E-05 | 5.20E-06 |
| SA5 | Run 7 | Run 6 | 9.05E-09 | 1.85E-08 | 6.07E-05 | 1.12E-05 |
| SA6 | Run 7 | Run 8 | 2.40E-08 | 4.98E-08 | 9.27E-05 | 1.85E-05 |
| 1Way1 | Run 33 | Run 31 | 1.03E-08 | 2.07E-08 | 5.32E-05 | 7.03E-06 |
| 1Way2 | Run 33 | Run 32 | 1.09E-08 | 2.20E-08 | 5.98E-05 | 9.73E-06 |
| 1Way3 | Run 33 | Run 34 | 1.21E-08 | 2.44E-08 | 6.34E-05 | 9.55E-06 |
| 2Way1 | Run 28 | Run 26 | 2.65E-06 | 5.42E-06 | 8.49E-04 | 2.82E-04 |
| 2Way2 | Run 28 | Run 27 | 1.47E-05 | 3.09E-05 | 2.21E-03 | 8.16E-04 |
| 2Way3 | Run 28 | Run 29 | 8.80E-06 | 1.86E-05 | 1.68E-03 | 6.20E-04 |
| 2Way4 | Run 15 | Run 13 | 1.12E-06 | 2.32E-06 | 4.76E-04 | 1.52E-04 |
| 2Way5 | Run 15 | Run 14 | 5.03E-06 | 1.05E-05 | 1.16E-03 | 3.78E-04 |
| 2Way6 | Run 15 | Run 16 | 1.89E-06 | 3.90E-06 | 6.66E-04 | 2.09E-04 |

**Table 4. Comparison statistics of the computed 2-D ADCIRC water surface elevation ($n$ = 20,601 and $n_t$ = 342)**

| Comparison ID | Compared Model Runs | | 1-ACOD | 1-ACOE | ARMSD | AMAD |
| | Reference Run | Comparative Run | | | | |
|---|---|---|---|---|---|---|
| SA1 | Run 3 | Run 1 | 0.00E+00 | 0.00E+00 | 3.13E-14 | 2.19E-16 |
| SA2 | Run 3 | Run 2 | 0.00E+00 | 0.00E+00 | 2.26E-13 | 1.58E-15 |
| SA3 | Run 3 | Run 4 | 0.00E+00 | 0.00E+00 | 1.82E-13 | 1.40E-15 |
| 1Way1 | Run 33 | Run 31 | 0.00E+00 | 0.00E+00 | 3.13E-14 | 2.19E-16 |
| 1Way2 | Run 33 | Run 32 | 0.00E+00 | 0.00E+00 | 2.26E-13 | 1.58E-15 |
| 1Way3 | Run 33 | Run 34 | 0.00E+00 | 0.00E+00 | 1.82E-13 | 1.40E-15 |
| 2Way1 | Run 28 | Run 26 | 4.54E-07 | 9.11E-07 | 2.67E-04 | 9.69E-05 |
| 2Way2 | Run 28 | Run 27 | 3.99E-06 | 7.99E-06 | 7.84E-04 | 3.03E-04 |
| 2Way3 | Run 28 | Run 29 | 2.19E-06 | 4.38E-06 | 5.75E-04 | 2.32E-04 |
| 2Way4 | Run 15 | Run 13 | 8.30E-08 | 1.67E-07 | 1.18E-04 | 4.15E-05 |
| 2Way5 | Run 15 | Run 14 | 5.58E-07 | 1.12E-06 | 2.83E-04 | 9.72E-05 |
| 2Way6 | Run 15 | Run 16 | 2.04E-07 | 4.09E-07 | 1.86E-04 | 6.34E-05 |

**Comparison among coupling schemes.** We compare results from the model runs associated with stand-alone, one-way coupling, and two-way coupling simulations when $\Delta t_{ADCIRC}$ = 1 s, $\Delta t_{channel}$ = 0.5 s, $\Delta t_{overland}$ = 5 s, $\Delta t_{subsurface}$ = 3 min, $\Delta t_{coupling}$ = 3 min, and the number of processors are 8 and 32 for ADCIRC and pWASH123D, respectively. That is, Run 3 (ADCIRC stand-alone), Run 11 (pWASH123D stand-alone), Run 33 (one-way coupling), and Run 28 (two-way coupling) are compared.

First, we compare the wall clock time of Runs 3, 11, 33, and 28 that can be extracted from Table 1 (Table 5). It is clear that when the number of processors was set to 32 for pWASH123D and 8 for ADCIRC, the performance bottleneck was on the pWASH123D computation for this Biloxi example. It should be noted that the wall clock time for two-way coupling (Run 28) is less than that for one-way coupling (Run 33) and much less than that for pWASH123D stand- alone (Run 11), though the pWASH123D processors were the same (i.e., 32) for these three runs. As we should expect, different coupling schemes will result in different water surface elevation values on the coupling interface. While pWASH123D solves nonlinear 1-D channel, 2-D overland, and 3-D subsurface equations, different water surface elevation values applied to the coastal line (i.e., the coupling interface) may require different numbers of nonlinear iterations to reach convergent solutions. The result shown in Table 5 suggests that the coupling simulation can be computationally more efficient than the pWASH123D stand-alone simulation with only a few extra processors employed for ADCIRC computation.

| Table 5. Wall clock time of Runs 3, 11, 33, and 28. | | | | |
|---|---|---|---|---|
| **Run ID** | **No of Proc.** | | **Wall Clock Time (s)** | **Simulation Type** |
| | **pWASH123D** | **ADCIRC** | | |
| 3 | 0 | 8 | 2,624 | ADCIRC stand alone |
| 11 | 32 | 0 | 10,205 | pWASH123D stand alone |
| 33 | 32 | 8 | 6,923 | One-Way Coupling |
| 28 | 32 | 8 | 5,921 | Two-Way Coupling |
| * Time-steps for base case simulation: $\Delta t_{ADCIRC}$ = 1 s; $\Delta t_{channel}$ = 0.5 s; $\Delta t_{overland}$ = 5 s; $\Delta t_{subsurface}$ = 3 min; $\Delta t_{coupling}$ = 3 min <br> ** Hydraulic conductivities for base case simulation: 100 m/hr (horizontal) and 10 m/hr (vertical) | | | | |

Tables 6 through 8 compare model run results among Runs 3, 11, 33, and 28. The values of the four deviation measures are much greater than those shown in Tables 2 through 4, indicating discrepancies between the compared model runs due to different coupling schemes. The four deviation measures have the smallest values associated with the computed 2-D ADCIRC water surface elevation and the largest values with the computed 1-D channel stage, indicating that when compared with the 2-D overland water depth and the 2-D ADCIRC water surface elevation, the 1-D channel stage is more sensitive to the switch from a coupling scenario (i.e., stand-along, one-way coupling, or two-way coupling) to another.

| Table 6. Comparison statistics of the computed 1-D channel stage among stand-alone, one-way coupling, and two-way coupling. | | | | | | |
|---|---|---|---|---|---|---|
| **Comparison ID** | **Compared Model Runs** | | **1-ACOD** | **1-ACOE** | **ARMSD, m** | **AMAD, m** |
| | **Reference Run** | **Comparative Run** | | | | |
| 2Way–SA | Run 28 | Run 11 | 6.21E-02 | 7.66E-01 | 1.03E-01 | 9.35E-02 |
| 2Way–1Way | Run 28 | Run 33 | 5.89E-02 | 7.00E-01 | 9.31E-02 | 8.44E-02 |
| 1Way-SA | Run 33 | Run 11 | 9.54E-03 | 1.67E-01 | 3.00E-02 | 2.63E-02 |

**Table 7. Comparison statistics of the computed 2-D overland water depth among stand-alone, one-way coupling, and two-way coupling.**

| Comparison ID | Compared Model Runs | | 1-ACOD | 1-ACOE | ARMSD, m | AMAD, m |
| | Reference Run | Comparative Run | | | | |
|---|---|---|---|---|---|---|
| 2Way–SA | Run 28 | Run 11 | 2.22E-03 | 6.38E-03 | 3.82E-02 | 1.66E-02 |
| 2Way–1Way | Run 28 | Run 33 | 1.66E-03 | 4.32E-03 | 3.34E-02 | 1.44E-02 |
| 1Way-SA | Run 33 | Run 11 | 6.47E-04 | 1.92E-03 | 1.37E-02 | 5.78E-03 |

**Table 8. Comparison statistics of the computed 2-D ADCIRC water surface elevation among stand-alone, one-way coupling, and two-way coupling.**

| Comparison ID | Compared Model Runs | | 1-ACOD | 1-ACOE | ARMSD, m | AMAD, m |
| | Reference Run | Comparative Run | | | | |
|---|---|---|---|---|---|---|
| 2Way–SA | Run 28 | Run 3 | 3.16E-04 | 7.13E-04 | 8.48E-03 | 3.17E-03 |
| 2Way–1Way | Run 28 | Run 33 | 3.16E-04 | 7.13E-04 | 8.48E-03 | 3.17E-03 |
| 1Way-SA | Run 33 | Run 3 | 0.00E+00 | 0.00E+00 | 0.00E+00 | 0.00E+00 |

Figures 12 and 13 depict the absolute differences of 1-D channel stage between model runs 11 (pWASH123D stand alone), 33 (one-way coupling), and 28 (two-way coupling). Figure 14 plots the absolute differences of 2-D overland water depth between the aforementioned model runs. Figure 12 shows that significant water stage differences exist between two-way coupling and the other two simulations during the storm period (36 – 56 hr). Channel water stage differences become minimal during quiet periods (0 – 36 and 56 – 72 hr). Moreover, upstream reaches have smaller stage differences than downstream reaches based on the channel reach distribution specified in Figure 9. Figure 13 shows that stage differences at Junctions 1 and 3 (Figure 9) between two-way coupling and stand-alone simulations are insignificant during quiet periods but can reach 0.6 m during the storm period. Figure 14 shows that the differences of overland water depth increased as the storm came and decreased as the storm left. All the three figures suggest that the coupling scheme has limited effect on watershed simulation results during non-storm periods. The discrepancies between the channel stage results from two-way and one-way coupling (Figure 12b) increase with the strength of the storm, suggesting that the greatest watershed-nearshore interaction is at the storm peak, which implies that one-way coupling will be insufficient in accounting for watershed-nearshore interaction when storms are greater than a certain degree.
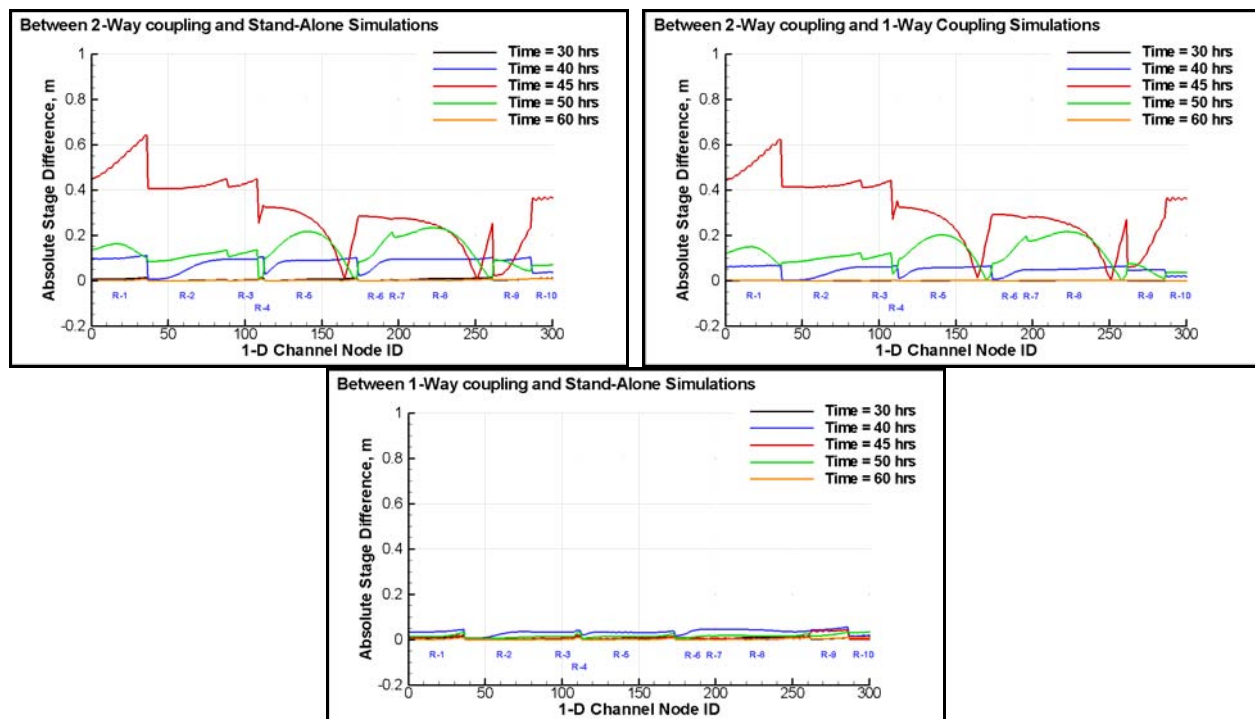
Figure 12.  Absolute differences of 1-D channel stage between (a) two-way coupling and stand-alone, (b) two-way coupling and one-way coupling, and (c) one-way coupling and stand-alone simulations at various times, where Reach R-1 contains Nodes 1-36, R-2 Nodes 37-88, R-3 Nodes 89-108, R-4 Nodes 109-112, R-5 Nodes 113-173, R-6 Nodes 174-196, R-7 Nodes 197-210, R-8 Nodes 211-261, R-9 Nodes 262-286, R-10 Nodes 287-301.
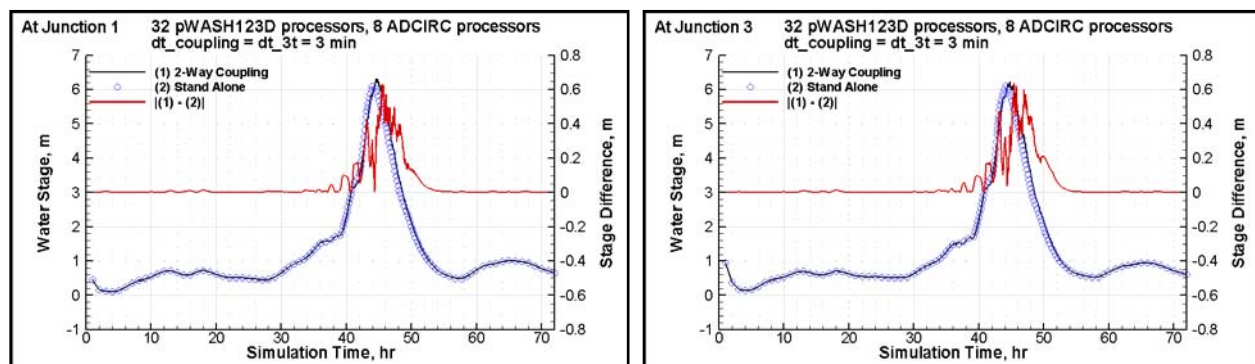


Figure 13.  Absolute differences of 1-D channel stage (in meter) between two-way coupling and stand-alone simulations at Junctions 1 (left) and 3 (right).
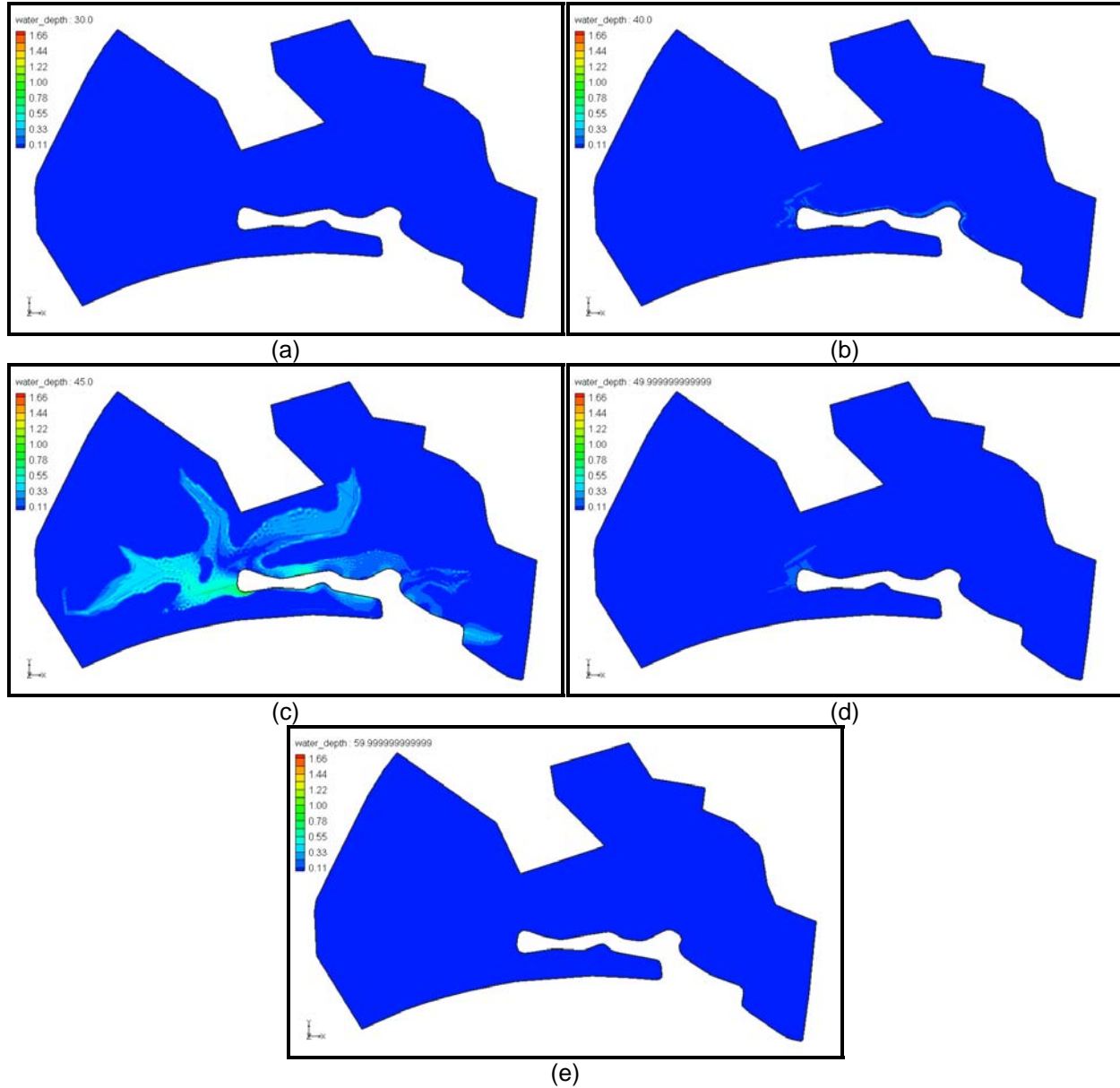
Figure 14. Absolute differences of overland water depth between two-way coupling and stand-alone simulation at the (a) 30th, (b) 40th, (c) 45th, (d) 50th, and (e) 60th hr.

Figure 15 presents the absolute differences of 2-D ADCIRC water surface elevation between two-way coupling (Run 28) and stand-alone (Run 3) simulations at various times. Significant differences occur in the Biloxi Bay during the storm event (Time = 45 hr). These differences decrease with the distance from the coastal line, indicating that the impact from pWASH123D to ADCIRC was mainly in the bay area and around the coastal line.
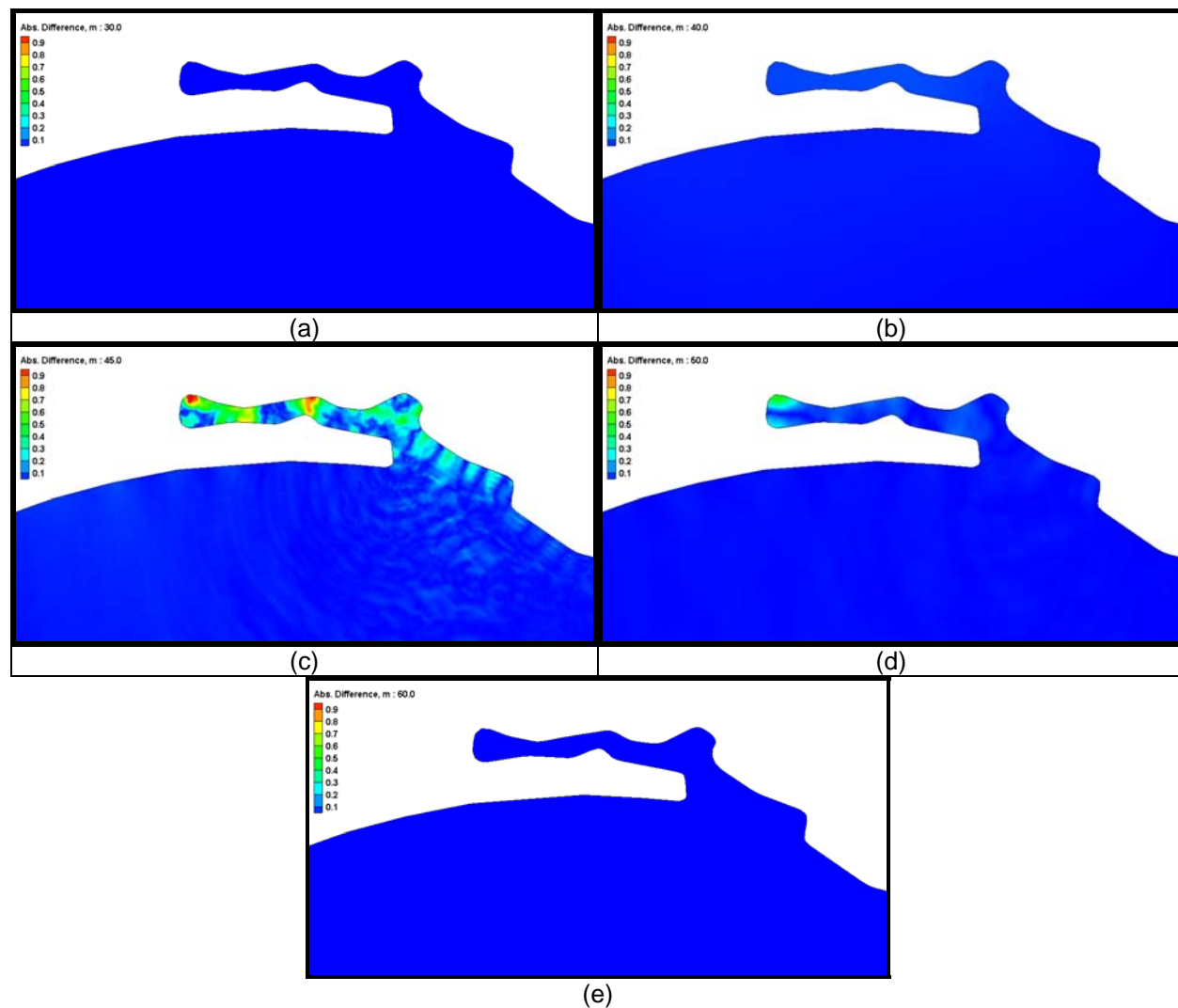
Figure 15.  Absolute differences of ADCIRC water surface elevation (in meter) between two-way coupling and stand-alone simulations at the (a) 30th, (b) 40th, (c) 45th, (d) 50th, and (e) 60th hr.

**Effect of time lagging**. Figures 16 and 17 present the absolute differences of overland water depth and ADCIRC water surface elevation between 3-min (Run 28) and 6-min (Run 25) coupling. The time lagging effect was insignificant except for at around the peak of the storm (i.e., time = 45 hr). The large lagging effect occurred mainly around channel exits, especially the exit of Biloxi River.
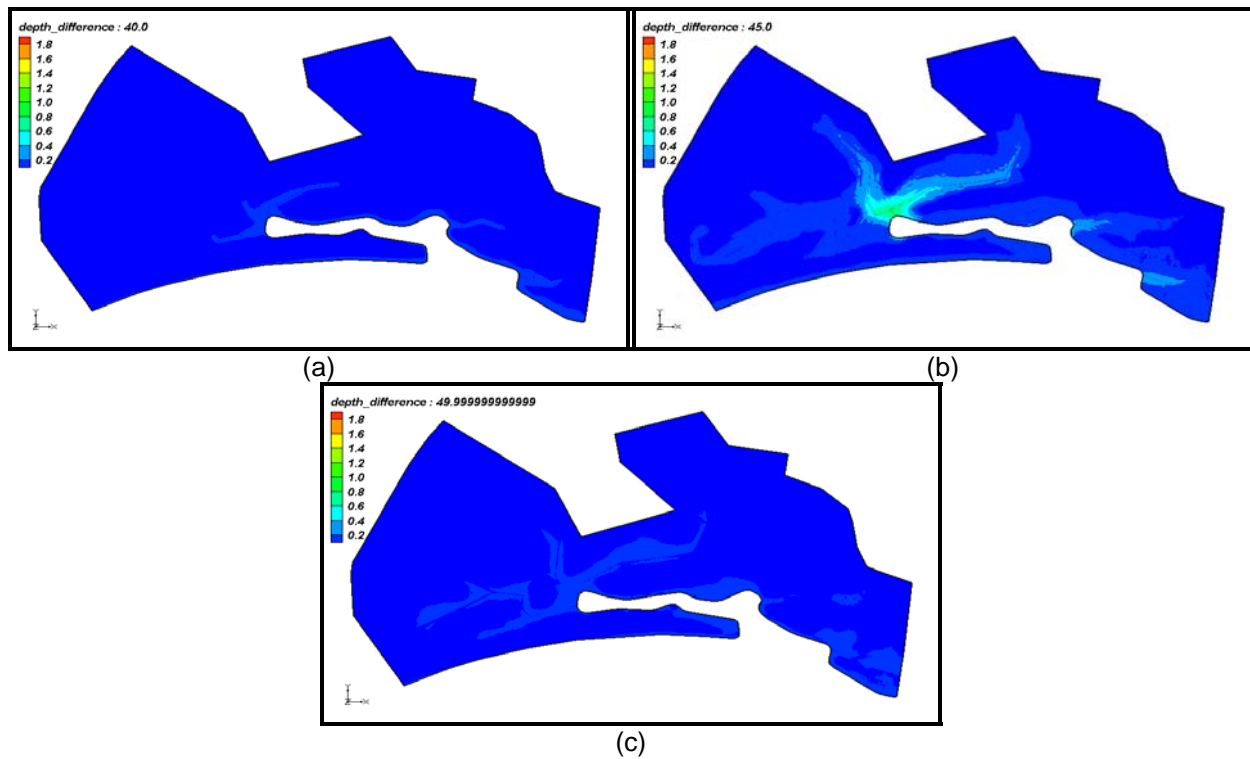
Figure 16.  Absolute differences of overland water depth (in meter) between 3-minute coupling and 6-minute coupling at the (a) 40th, (b) 45th, and (c) 50th hr.
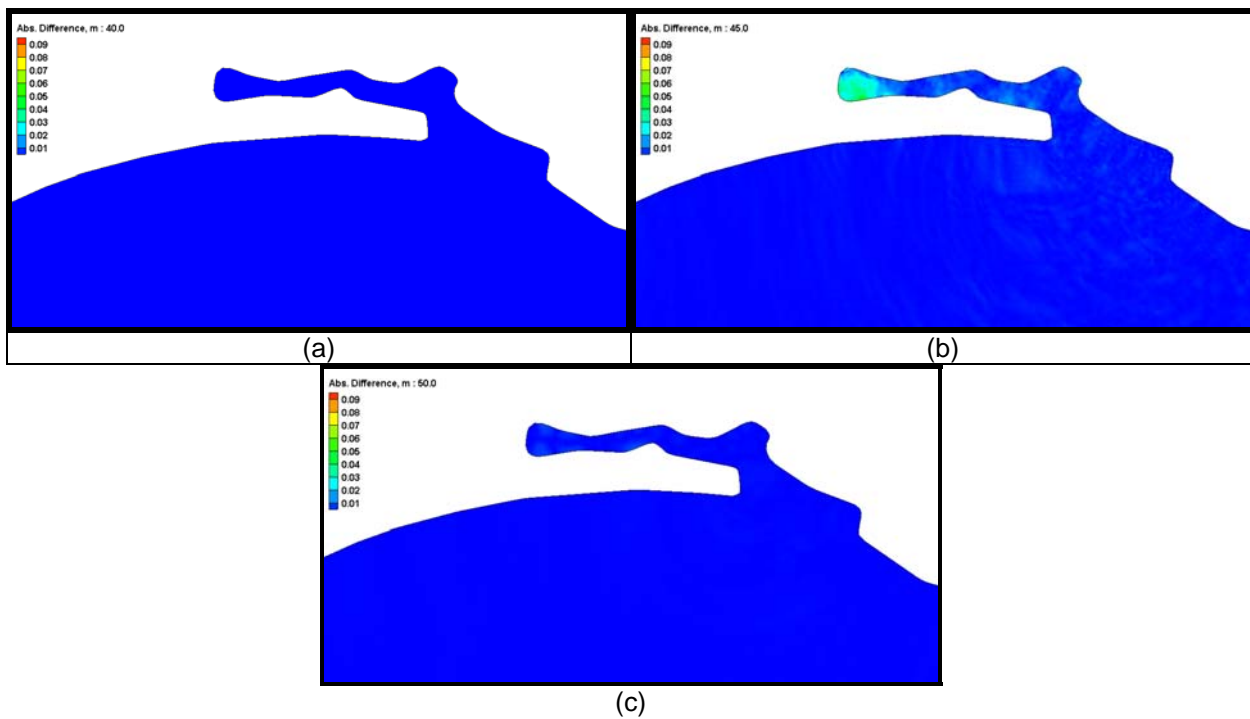


Figure 17.  Absolute differences of ADCIRC water surface elevation (in meter) between 3-minute coupling and 6-minute coupling at the (a) 40th, (b) 45th, and (c) 50th hr.

**Effect of hydraulic conductivity**. For a demonstration purpose, there were only two subsurface materials considered in this simplified Biloxi model: fine sand along channels and sand elsewhere. The horizontal/vertical hydraulic conductivities (K) for sand and fine sand were set to 100/10 and 10/1 m/hr, respectively, for the base case (Table 1) and the subsurface domain. Figure 18 shows the differences of ADCIRC water surface elevation between the base case (i.e., Run 28) and when the K values are 10 times those of the base case (i.e., Run 19). On the other hand, Figure 19 presents the water surface elevation differences between the base case and when the K values are 1/10 of the base case (i.e., Run 23). When K is 10 times those of the base case values, large differences of water surface elevation exist in the bay area during the storm period. This is because larger K directs to greater surface-subsurface interaction, which promotes significant water exchange between watershed and nearshore models when a storm is the driving force for water movement. On the other hand, smaller K implies less surface-subsurface interaction and a smaller contribution to the flux across the coupling interface of the watershed-nearshore model.
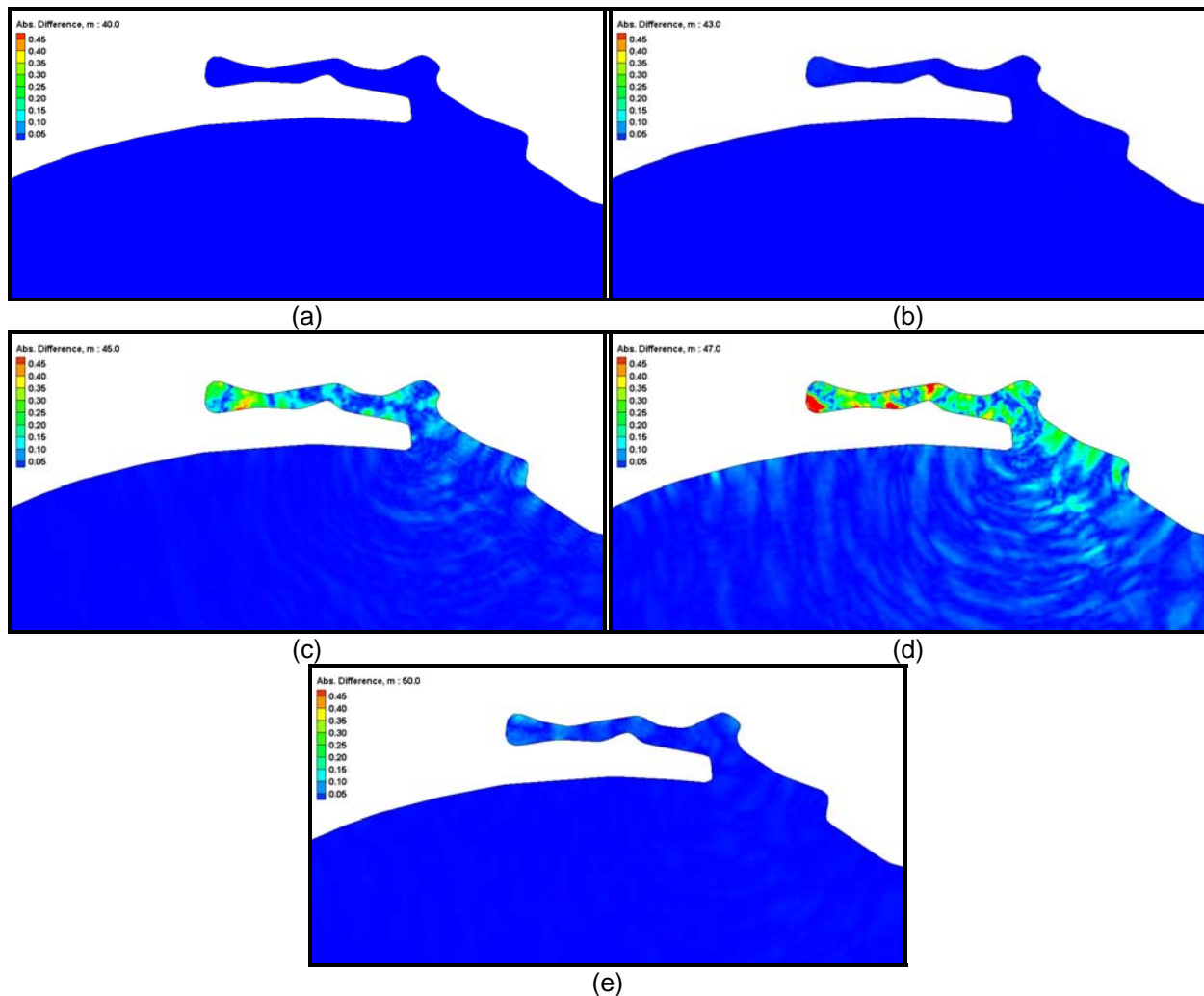


Figure 18.  Absolute differences of ADCIRC water surface elevation (in meter) between Run 28 (base case, K = $K_{base}$) and Run 19 (K = 10x$K_{base}$) at the (a) 40th, (b) 43rd, (c) 45th, (d) 47th, and (e) 50th hr.
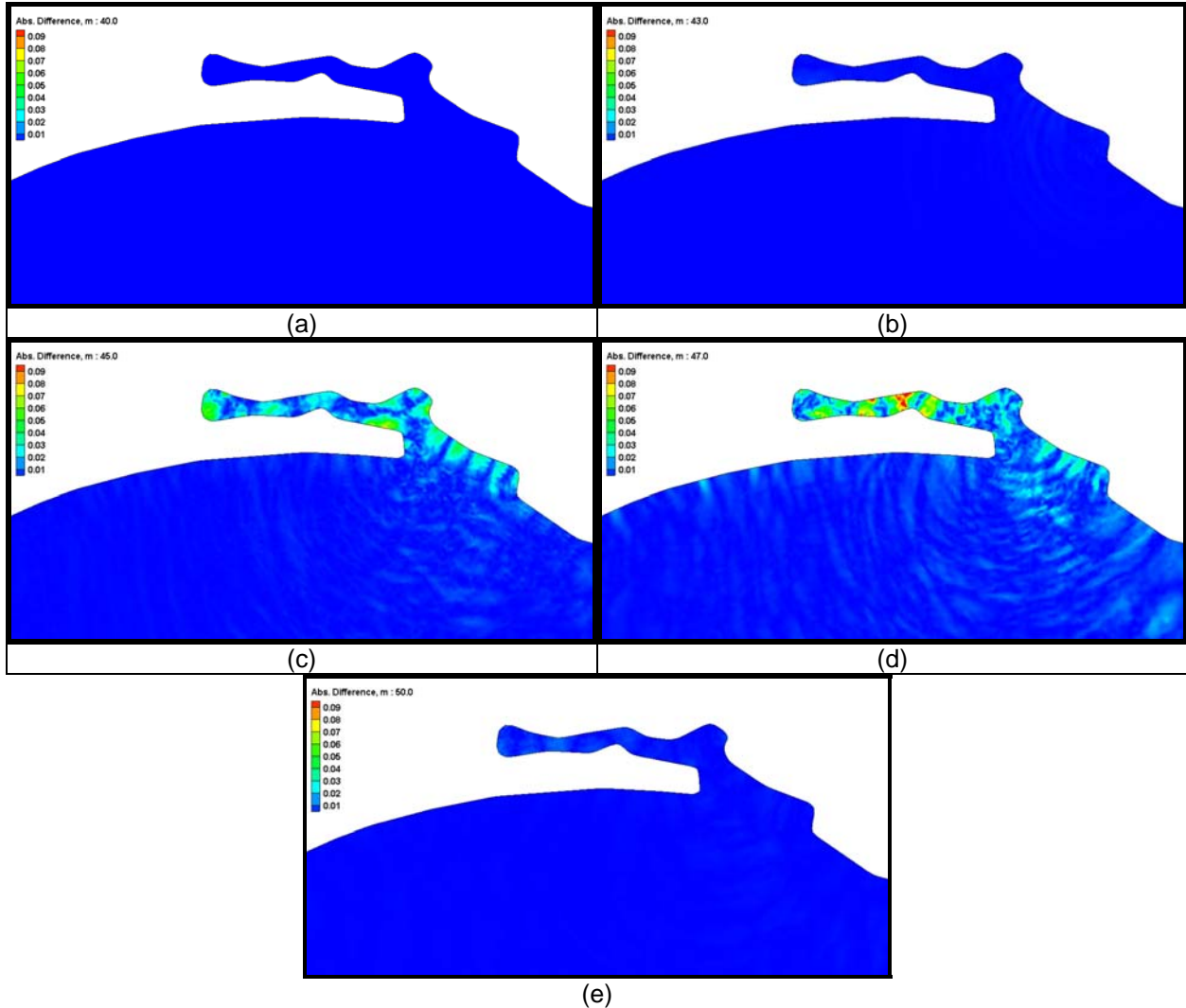
Figure 19. Absolute differences of ADCIRC water surface elevation (in meter) between Run 28 (base case, K = K$_{base}$) and Run 23 (K = 0.1xK$_{base}$) at various times: 40, 43, 45, 47, and 50 hr (left to right).

**SUMMARY AND FUTURE PLAN:** In this technical note, a coupled watershed-nearshore model newly developed in the BEI was presented as a research demonstration project under the support of SWWRP. The model coupled pWASH123D and ADCIRC through ESMF and DBuilder. The pWASH123D and ADCIRC models were currently coupled in a concurrent model with time lagging, and the coupling interface was the coastal line. A simplified Biloxi Bay model was constructed for demonstration. This Biloxi Bay model used historical data as well as the simulation result from a large-scale 2-D ADCIRC simulation of hurricane Katrina as the driving forces for water movement. GMS 6.5 was used to produce the pWASH123D input files and the ADCIRC domain geometry (mesh) files. By using GMS, we can ensure that the pWASH123D and ADCIRC interface boundary nodes truly sit on the coupling interface, which is essential for element searching.

This task included 38 model runs to examine parallel efficiency, accuracy, and impacts from coupling scheme, time lagging method, and assumed hydraulic conductivity. Through the analysis of the model run results, the following were observed.

- The most significant impact from coupling ADCIRC to pWASH123D was on the areas around the coastal line near shallow water areas and the channels.

- The most significant impact from coupling pWASH123D to ADCIRC was on the bay area and around the coastal line.

- The time lagging effect became significant during storm events, suggesting that higher coupling frequency should be used during these periods of time.

- Large hydraulic conductivity implies great surface-subsurface interaction and subsequently promotes water exchange between the watershed and nearshore models.

- When compared with the 2-D overland water depth and the 2-D ADCIRC water surface elevation, the 1-D channel stage is more sensitive to coupling scenarios (i.e., stand-alone, one-way coupling, or two-way coupling).

- Two-way coupling is necessary to accurately account for watershed-nearshore interaction during storm events.

- The coupled pWASH123D-ADCIRC model provides consistent computational results in stand-alone, one-way coupling, and two-way coupling simulations when the number of processors varies.

- The coupling simulation can be computationally more efficient than the pWASH123D stand-alone simulation with only a few extra processors employed for ADCIRC computation (e.g., two-way coupling Runs 15 and 28 versus stand-alone Runs 7 and 11, respectively). In-depth investigation for this is needed to determine the reason(s).

- For this simplified Biloxi Bay model, using 32 pWASH123D processors and 8 ADCIRC processors was the best combination for the designated 72-hour simulation when both the PE and wall clock time are considered.

The coupled model in the current form can be used to model water flow in combined watershed-nearshore systems. Using high performance computing produces the spatial distributions of water flow and head in the combined system at designated time-steps. The coupled model can help better understand both the surface-subsurface and the watershed-nearshore interactions as well as construct and verify adequate plans for water management and other water-related environmental issues.

The coupled pWASH123D-ADCIRC model is the first coupled unstructured-mesh model using ESMF. Features and capabilities developed for this coupled model can also be applied to the coupling of structured- and unstructured-mesh models. When compared to stand-alone models, the coupled model exhibits more accurate boundary conditions applied to the interface boundary between the watershed and the coastal models, especially when surface-subsurface and watershed-coastal ocean interactions are significant during storm events. As a result, the hydro-system in the nearshore area has been modeled better, and an improved understanding of the complex interactions can be obtained. The future improvement/development may include the following.

- Incorporate temporal interpolation to reduce the time lagging effect.

- Implement the coupling through overlapped wetting-drying areas and extend the subsurface domain to some distances off the coastal line.

- Develop salinity transport and density-dependent flow capabilities in the coupled model.

- Make the watershed-nearshore coupling time-step a factor, rather than a multiple, of the 3-D subsurface time-step.

## ADDITIONAL INFORMATION:

This work was funded by the SWWRP. At the time of publication, the SWWRP Program Manager was Dr. Steven L. Ashby: *Steven.L.Ashby@usace.army.mil*. Dr. Jeffery Allen (ITL) and Aaron Byrd reviewed this technical note.

This technical note should be cited as follows:

Cheng, H.-P., J.-R. C. Cheng, R. M. Hunter, and H.-C. Lin. 2010. *Demonstration of a coupled watershed-nearshore model.* ERDC TN-SWWRP-10-XX. Vicksburg, MS: U.S. Army Engineer Research and Development Center. *https://swwrp.usace.army.mil/.*

## REFERENCES:

ADCIRC. 2009. ADCIRC Coastal Circulation and Storm Modeling. *http://adcirc.org/index.html*

Bonet, J., and J. Peralie. 2005. *An alternating digital tree (ADT) algorithm for 3D geometric searching and intersection problems*. International Journal for Numerical Methods in Engineering 31(1), 1-17.

Bunya, S., J. C. Dietrich, J. J. Westerink, B. A. Ebersole, J. M. Smith, J. H. Atkinson, R. Jensen, D. T. Resio, R. A. Luettich, C. Dawson, V. J. Cardone, A. T. Cox, M. D. Powell, H. J. Westerink, and H. J. Roberts. 2010a. *A high-resolution coupled riverine flow, tide, wind, wind wave, and storm surge model for southern Louisiana and Mississippi. Part I: Model development and validation.* Monthly Weather Review 138(2), 345-377.

Bunya, S., J. C. Dietrich, J. J. Westerink, B. A. Ebersole, J. M. Smith, J. H. Atkinson, R. Jensen, D. T. Resio, R. A. Luettich, C. Dawson, V. J. Cardone, A. T. Cox, M. D. Powell, H. J. Westerink, and H. J. Roberts. 2010b. *A high-resolution coupled riverine flow, tide, wind, wind wave, and storm surge model for southern Louisiana and Mississippi. Part II: Synoptic description and analysis of Hurricanes Katrina and Rita.* Monthly Weather Review 138(2), 345-377.

Cheng, J-R. C., R. M. Hunter, H-P. Cheng, D. R. Richards, and G-T. Yeh. 2006. *Parallelization of a watershed model-phase III: Coupled 1-dimensional channel, 2-dimensional overland, and 3-dimensional subsurface flows.* Computational Methods in Water Resources XVI (CMWR XVI), in proceedings CD-ROM, 19-22 June 2006, Copenhagen, Denmark.

Cheng, J-R. C., H-P. Cheng, H-C. Lin, R. M. Hunter, D. R. Richards, and E. V. Edris. 2007. *A Performance Study of Parallel Algorithms in pWASH123D*. World Water and Environmental Resources Congress, in *Proceedings* CD-ROM, 15-19 May 2007, Tampa, FL, USA.

Department of Defense. 2010. DOD High Performance Computing Modernization Program. *http://www.hpcmo.hpc.mil/cms2/index.php/institutes*

ESFM. 2009. Earth Systems Modeling Framework. *http://www.esmf.ucar.edu/*

Hunter, R. M., and J-R. C. Cheng. 2005. *DBuilder: A parallel data management toolkit for scientific applications*. In *Proceedings of the 2005 International Conference on Parallel and Distributed Processing Techniques and Applications (PDPTA'05)*, CSREA Press, Las Vegas, Nevada, 825-831.

U.S. Army Corps of Engineers. 2009. GMS-Groundwater Modeling System. *http://chl.erdc.usace.army.mil/gms*

Yeh, G.-T., G. Huang, H.-P. Cheng, F. Zhang, H.-C. Lin, E. Edris, and D. Richards. 2006. *A first-principle, physics-based watershed model: WASH123D. Watershed models*. ed. V. P. Singh and D. K. Frevert. CRC Press, Taylor and Francis Group.